Enhanced Generation of Reactive Species by Cold Plasma in Gelatin Solutions for Selective Cancer Therapy

Journal:	*ACS Applied Materials & Interfaces*
Manuscript ID	Draft
Manuscript Type:	Article
Date Submitted by the Author:	n/a
Complete List of Authors:	Labay, Cedric; Universitat Politecnica de Catalunya Roldan, Marcel; Universitat Politecnica de Catalunya Tampieri, Francesco; Universitat Politecnica de Catalunya, Department of Materials Science and Metallurgy Stacampiano, Augusto; GREMI Escot Bocanegra, Pablo; GREMI Ginebra, Maria-Pau; Universitat Politecnica de Catalunya, Department of Materials Science and Metallurgical Engineering Canal, Cristina; Universitat Politecnica de Catalunya, Materials Science and Engineering Department

Enhanced Generation of Reactive Species by Cold Plasma in Gelatin Solutions for Selective Cancer Therapy

Cédric Labay[1,2,3], Marcel Roldán[1,2], Francesco Tampieri[1,2,3], Augusto Stancampiano[4], Pablo Escot Bocanegra[4], Maria-Pau Ginebra[1,2,3,5], Cristina Canal[1,2,3]

[1] Biomaterials, Biomechanics and Tissue Engineering Group, Universitat Politècnica de Catalunya (UPC), Av. Eduard Maristany 10-14, 08019 Barcelona, Spain

[2] Barcelona Research Center in Multiscale Science and Engineering, UPC, Barcelona, Spain

[3] Research Centre for Biomedical Engineering (CREB), UPC, 08019 Barcelona, Spain

[4] GREMI, UMR 7344, CNRS/Université d'Orléans, BP 6744, CEDEX 2, 45067 Orléans, France

[5] Institute for Bioengineering of Catalonia (IBEC), c/ Baldiri i Reixach 10-12, 08028 Barcelona, Spain

Corresponding author: cristina.canal@upc.edu

ABSTRACT

Atmospheric pressure plasma jets generate reactive oxygen and nitrogen species (RONS) in liquids and biological media, which find application in the new area of plasma medicine. These plasma-treated liquids demonstrated recently to possess selective properties on killing cancer cells and attract attention towards new plasma-based cancer therapies. These allow for local delivery by injection in the tumor but can be quickly washed away by body fluids. By confining these RONS in a suitable biocompatible delivery system, great perspectives can be opened in the design of novel biomaterials aimed for cancer therapies. Gelatin solutions are evaluated here to store RONS generated by atmospheric pressure plasma jets, and their release properties are evaluated. The concentration of RONS was studied in 2% gelatin as a function of different plasma parameters (treatment time, nozzle distance and gas flow) with two different plasma jets. Much higher production of reactive species (H_2O_2 and NO_2^-) was revealed in the polymer solution than in water after plasma treatment. The amount of RONS generated in gelatin is greatly improved with respect to water, with concentrations of H_2O_2 and NO_2^- between 2 and 12 times higher for the longest plasma treatments. Plasma-treated gelatin exhibited the release of these RONS to a liquid media, which induced an effective killing of bone cancer cells. Indeed, *in vitro* studies on Sarcoma Osteogenic (SaOS-2) cell line exposed to plasma-treated gelatin lead to time-dependent increasing cytotoxicity with the longer plasma treatment time of gelatin. While SaOS-2 cell viability decreased down to 12%-23% after 72 hours for cells exposed to 3-min treated gelatin, viability of healthy cells (hMSC) was preserved (around 90%), establishing the selectivity of the plasma-treated gelatin on cancer cells. This sets the basis for designing improved hydrogels with high capacity to deliver RONS locally to tumors.

Keywords: Cold atmospheric plasma; hydrogel; osteosarcoma; reactive oxygen and nitrogen species.

1. INTRODUCTION

The potential of targeting the oxidative stress response in cancer cells that could overcome drug resistance and spare normal tissue is being investigated as novel treatment by different techniques. Production of reactive oxygen and nitrogen species (RONS) in liquids (water, saline solutions, cell culture media) by treatment with cold atmospheric plasmas has been focus of interest in the last years due to its implications in biology and medicine (i.e. from wound healing to cancer treatment). Thus, the generation of species such as H_2O_2, NO_2^-, O_3^- or short-lived species has been extensively described [1–4]. The plasma-treated or plasma-conditioned liquids (PCL) with biological effects provide a new window of opportunities for local treatment by injecting in the disease site. Taking advantage of the different basal levels of oxidative stress between healthy and cancer cell lines[5–8], and the different sensitivity to reactive oxygen species (ROS), previous works demonstrated the selective effects of PCL on killing cancer cells[9–15]. However, injection of PCL to the tumor may quickly be washed away by body fluids, so design of suitable biomaterials for delivery of these oxidative stress is of paramount importance. In this sense, and to also foster higher concentrations of RONS in suitable biocompatible vehicles studies on PCL were broadened to alginate solutions, that proved to be good candidates to enhance generation of RONS [16]. Therefore, developing vehicles of these RONS for enhanced local delivery to the diseased site would be a very interesting asset.

Gelatin is a translucid and thermosensitive hydrogel derived from collagen. Since collagen is the most abundant extracellular matrix protein in humans and animals, and the main component of connective tissues (such as skin, ligament, tendons, etc.), gelatin presents a high biocompatibility, making it a great candidate to be used in the design of hydrogel-based implantable biomaterials. Indeed, as biomaterials for tissue engineering, a wide diversity of gelatin-based structures have been described in literature[17] including nano- and micro-spheres[18,19] or particles, 3D scaffolds[20–24], electrospun nanofibers[25–27], cryogel scaffolds[28], composite materials[29–31] and *in situ* gelling formulations. This reverts in a broad range of applications going from drug and growth factors delivery[18,19,30] to tissue repair and regeneration for ocular[23], bone[30], skeletal muscle[32] or soft tissue[24,31] engineering.

The first studies involving cold atmospheric plasma treatment of gelled gelatin used it as a surrogate of human tissues – i.e. skin - to study its barrier effects on incoming RONS generated by different kinds of plasma treatment (plasma jet, barrier discharge). The penetration of RONS through gelatin gel films was quantified measuring the concentrations in the water underneath such films[33–35]. Other materials such as agarose[36] and phospholipid membranes[37] were employed to model living tissues, where the authors also focused on the transport and diffusion of the RONS through these layers.

Here, we intend to describe for the first time the ability of gelatin solutions to successfully increase, store and deliver reactive species generated by cold atmospheric plasmas with the purpose to further include the plasma-treated biopolymer in the design of hydrogel-based biomaterial acting as vehicles of RONS for cancer therapy. A wide variety of plasma jets have been described, producing different biological effects, so here focus will be put on comparing a helium atmospheric pressure plasma jet (APPJ) to a standard commercial source argon jet (known as kINPen) on the production of RONS in gelatin and investigating its potential biological effects.

2. EXPERIMENTAL SECTION

2.1. Materials

Gelatin type B (Rousselot 250 LB8, Rousselot, France), in powder form and MilliQ water (MilliPore, Merck) (designated here as DI water) were used for preparation of biopolymer solution. Argon (Ar 5.0) and Helium (He 5.0) employed as precursor gas to generate plasma (PRAXAIR, Spain).

Sulfanilamide (Sigma-Aldrich, USA), N-(1-naphthyl)ethylenediamine dihydrochloride (Sigma-Aldrich, USA) and ortho-phosphoric acid 85%, pure, pharma grade (H_3PO_4) (85%) (Panreac, USA) have been used for the preparation of Griess reagent, used for NO_2^- detection. Sodium nitrite ($NaNO_2$, Sigma-Aldrich, USA) used for calibration curves of nitrites. Sodium azide (NaN_3), Titanium(IV) oxysulfate-sulfuric acid solution ($TiOSO_4$) and 30% (w/w) hydrogen peroxide (H_2O_2) solution used for detection of hydrogen peroxides in water were purchased from Sigma Aldrich. Amplex™Red reagent (Invitrogen™, Thermo Fisher Scientific) and peroxidase from horseradish (Type VI) (HRP) (Sigma-Aldrich, USA) were used for determination of H_2O_2 in gelatin.

Nunclon™ Delta Surface 24-well and 96-well plates (ThermoFisher Scientific) and Corning® Transwell® polyester membrane cell culture inserts 6.5 mm Transwell® with 0.4 µm pore polyester membrane insert, TC-treated, sterile (Corning, Inc., USA) were used for *in vitro* cell experiments. Sarcoma osteogenic SaOS-2 (HTB-85, #70014245, ATCC, USA) were cultured in Mc Coy´s 5A medium (modified, with sodium bicarbonate, without L-glutamine, liquid, sterile-filtered, suitable for cell culture), purchased from Sigma Aldrich. Bone marrow-derived Mesenchymal Stem Cells hMSC (PCS-500-012, #70014245, ATCC, USA) were cultured in Advanced Dulbecco's Eagle Medium (1X) (AdvDMEM) (Gibco, ThermoFisher Scientific). To supplement cell culture media, Foetal Bovine Serum (FBS), Penicillin/Streptomycin (P/S) and Trypsin were purchased from ThermoFisher Scientific. Dulbecco's Phosphate Buffered Saline (PBS) used for *in vitro* cell assay and release experiments were obtained from Biowest (Biowest SAS, France). For sample preparation for confocal microscopy, Tween 20 (Sigma-Aldrich), SuperBlock™ (TBS) (ThermoScientific, Ref. 37535, USA) Alexa Fluor® 546 Phalloidin (Invitrogen™), ProLong® Gold antifade with DAPI (Invitrogen™, P36931, USA) were used.

2.2. Preparation of gelatin solution

Gelatin in powder form was mixed with MilliQ water at 37 ^oC using magnetic stirring for 2 hours to obtain a 2% $_{wt/wt}$ gelatin solution. 2% gelatin solution was stored at 4 ^oC and brought to 37 ^oC before plasma treatment.

2.3. Plasma treatment

In his work, two plasma sources were employed: an APPJ, using helium as plasma gas and whose design is based on a single electrode as described in literature[38] and a commercial kINPen® IND (NEOPLAS Tools, Germany)[39] operating with argon. Plasma treatment times up to 5 minutes were performed to either water or gelatin solutions. Nozzle distance to the solution surface was tested from 10 mm to 20 mm. Gas flow, controlled by Ar and He Bronkhorst Mass View flow controllers (Bronkhorst®, Netherlands), was employed between 1 and 5 L/min for APPJ and 1 and 2.5 L/min for kINPen due to the different configurations of the two plasma jets. To evaluate

the effects of APPJ and kINPen plasma treatment conditions on the amount of RONS generated in gelatin solution and the ageing of RONS, 200 µL of 2% gelatin solution previously warmed at 37 ^{o}C were put for treatment in a 96-well plate on a dielectric plate at floating potential **Error! Reference source not found.**(ungrounded samples). MilliQ water has been used as control in the same conditions.

2.4. pH monitoring

2 mL of 2 % gelatin solution brought to 37 ^{o}C were put in 24-well plates and treated with APPJ or kINPen at 10 mm nozzle distance and 1 L/min gas flow. Evolution of the pH as a function of plasma treatment time was measured by using a PC80 Multiparameter instrument (XS Instruments, Italy) with a Crison 50 14 electrode (Crison, Spain).

2.5. Infrared imaging of plasma-treated gelatin solution

Non-invasive temperature measurements were effectuated by means of an infrared camera (Fluke Ti480 by Fluke) with resolution of 640x640 pixels and an accuracy of ±2 °C. An initial calibration of the camera acquisition was effectuated using a standard thermocouple to measure the target temperature by contact. The emissivity was corrected with the calibration procedure. The camera was mounted 15 cm above the sample and focused on the sample surface. The acquisitions are reported on a scale from 10 to 40 °C so to accentuate the temperature gradients.

2.6. Detection of RONS

Quantification of plasma generated NO_2^- in 2% of gelatin solutions and in DI water was performed by Griess test[1,4,40,41]. Griess reagent (GR) was prepared by dissolution of 0.1 % $_{wt/v}$ of N-(1-naphthyl) ethylenediamine dihydrochloride, 1 % $_{wt/v}$ of sulphanilamide, and 5 % $_{wt/v}$ of phosphoric acid in DI water. 200 µL of GR were added on the 200 µL of plasma-treated sample in a 96-well plate (Figure 2a). Incubation of the plate protected from light was done for 10 min at room temperature before absorbance measurement at λ = 540 nm using a Synergy HTX Hybrid Multi Mode Microplate Reader (BioTek Instruments, Inc., USA). Calibration curves to correlate absorbance with concentration were made from $NaNO_2$ standard solutions with proper dilutions.

Quantification of plasma generated H_2O_2 in 2% gelatin solution or in water was performed by fluorescence measurement from the conversion of H_2O_2 in resorufin (fluorescent product) using 100 µM Amplex^{TM}Red reagent with 0.25 U/mL HRP as catalyst. The plasma-treated 2% gelatin solution samples were diluted 1:200 to proceed to the detection of H_2O_2 within the linear concentration range. 50 µL of the reagent were added to 200 µL of the diluted samples in a 96-well plate and that was incubated at 37 ^{o}C for 30 min. Fluorescence measurements were performed using a Synergy™ HTX Multi-Mode Microplate Reader (Biotek, USA) using 560/20 nm and 590/20 nm as filters for excitation and emission wavelengths, respectively.

2.7. Stability of RONS

The time stability of H_2O_2 and NO_2^- after storage of the plasma-treated 2% gelatin solution was measured following the protocol previously described, for each of the species. Gelatin solutions was stored either at 4 ^oC or 37 ^oC. DI water was used as control.

2.8. Release of RONS from plasma-treated hydrogels

200 µL of 2% gelatin solution were treated by APPJ or kINPen in 96-well plate at 10 mm with gas flow rate of 1 L/min during 30, 90 and 180 s. Then, plasma-treated gelatin samples, together with untreated gelatin as control, were transferred into Corning® Transwell® cell culture inserts and placed in 1 mL of PBS used as release medium in 24-well plates. Release kinetics of RONS from the gelatin to the PBS were plotted from withdrawals of 100 µL of the release medium at determined time points. 50 µL were used for NO_2^- and 50 µL for H_2O_2 detection, following the same experimental protocol described for RONS detection in DI water. 100 µL of fresh PBS at 37 ˚C were replaced after each sample withdrawal. At the end of the release experiments, final volumes of the release media were measured to consider any water evaporation. Thus, two volume corrections were taken into account to determine precisely the concentration RONS in the release medium at each moment t: (i) a step to step correction due to sample withdrawal and (ii) a total volume correction due to evaporation. Gelatine solutions were treated by plasma immediately before starting the RONS release experiments (without any storage time).

2.9. *In vitro* cell experiments

Sarcoma osteogenic SaOS-2 cells were used to evaluate the cytotoxicity of the plasma-treated 2% gelatin solutions on cancer cells. Cell culture medium of SaOS-2 consisted of Mc Coy´s 5A medium supplemented with 10% FBS and 1% P/S. Subconfluent SaOS-2 were detached from the flask using trypsin, centrifuged and seeded with a density of 10000 cells/well in 24-well plates with 1 mL volume of complete cell culture medium. After 6-hour adhesion, plasma-treated 2% gelatin solution samples were transferred to Transwell® inserts and placed in the wells. Gelatin solution used for cell experiments was previously heated at 37 ^oC and filtered with 0.22 µm-diameter pore Millex-GP filters (Millipore, Merck) before plasma treatment. Plasma treatments of the 2% gelatin solution used for in vitro cell experiments were performed with APPJ or kINPen for 30, 90 and 180 s using a 10 mm nozzle distance and 1 L/min gas flow rate. The same density of cells was seeded in the same conditions in empty well (cell only) and in presence of untreated gelatin, as controls. The cells were grown at 37 ^oC for another 24 and 72 hours.

Bone marrow-derived Mesenchymal Stem Cells (hMSC) were used to evaluate the selectivity of plasma-treated gelatin between cancer and healthy cell lines. Cell culture medium of hMSC consisted of AdvDMEM supplemented with 10% FBS and 1% P/S. Seeding, cell density and experimental design of hMSC were reproduced in the exact same conditions such as presented above with SaOS-2. hMSC cell viability was evaluated at 72 hours for cells in presence of untreated gelatin (control), APPJ- or kINPen-treated 2% gelatin solutions for the longest plasma treatment studied (180 s).

Cell viability at 24 and 72 hours was evaluated with WST-1 reagent following supplier's protocol. Absorbance was measured at λ_{abs} = 440 nm using a Synergy HTX Hybrid Multi Mode Microplate Reader (BioTek Instruments, Inc., USA). Normalization of the absorbance values was made with respect to cells only to determine the effects of untreated and plasma-treated 2% gelatin solution on SaOS-2 cell viability. Cell viability was also assessed by imaging the well plates by optical microscopy to check the coherence of the results.

2.10. Confocal Laser Scanning Microscopy

SaOS-2 cells were seeded on round glass slides in the bottom of a 24-well plate with a density of $3.0x10^4$ cells per well in 1 mL of McCoy´s 5A medium supplemented with 10% FBS and 1% P/S. After 6-hour adhesion, plasma-treated gelatin samples were transferred to Transwell® inserts and placed in the wells. The same density of cells was seeded in the same conditions without adding gelatin, as positive control. After 48 hours, SaOS-2 cells were fixed with 4% paraformaldehyde (PFA)/DPBS for 30 min at room temperature, 3x washed with PBS, and permeabilized with 0.1% Tween20/PBS during 30 min. They were washed three times with PBS and non-specifically points were blocked using SuperBlock™ (TBS) for 2 h. Then, cells were 3x washed and actin filaments were labelled using Alexa Fluor® 546 Phalloidin (AF546)/PBS in a dilution 1:300 to discern the cytoskeleton. After 1-hour incubation, samples were washed three times with PBS, and mounted using ProLong® Gold antifade with DAPI, allowing nuclei staining. SaOS-2 cells were imaged with a Zeiss LSM 800 Confocal Laser Scanning Microscope (CLSM) and processed with ZEN 2.3 software (Zeiss, Germany). Immunofluorescence images were taken using a 40x oil objective, using 557 nm and 353 nm as excitation wavelengths and 560-700 nm and 400-555 nm as detection wavelengths for AF546 and DAPI, respectively.

2.11. Data analysis

Statistical differences were determined using one-way ANOVA a 95% confidence with Tukey's post-tests using Minitab 19 software (Minitab, Inc., State College, PA). Statistical significance was noted when $p<0.05$.

3. RESULTS

3.1. Thermal effects of cold atmospheric plasma treatment

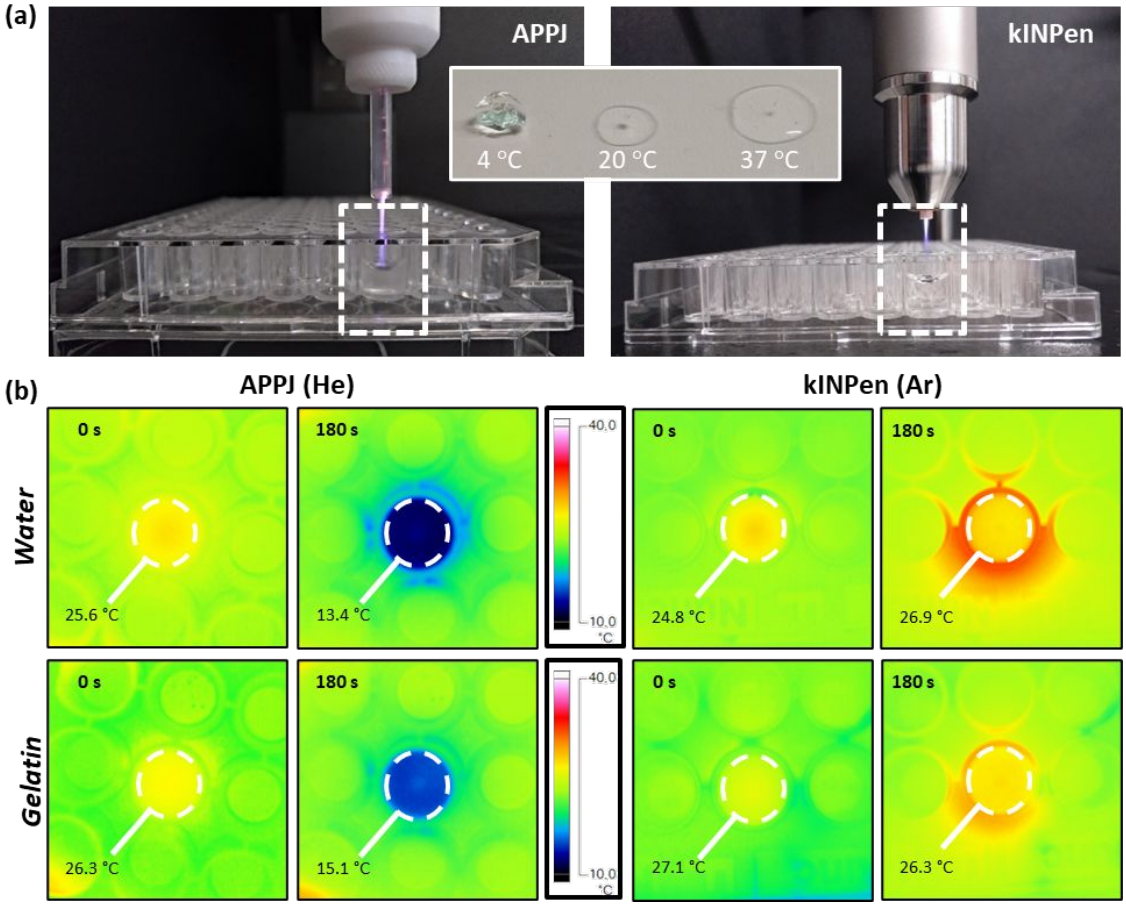

Figure 1: Configuration of the plasma treatment of gelatin using an APPJ and kINPen (a) together with the physical aspect of gelatin as function of temperature (inset). Thermal effects after 180 s of plasma treatment of water or 2% gelatin solution using APPJ and kINPen (10 mm, 1 L/min) monitored by infrared camera. The temperature value is calculated as an average over the gelatine surface (b).

Plasma treatments of 200 µL gelatin solution and water have been performed using APPJ and kINPen. The temperature of the solution was measured by IR imaging before and after plasma treatment and comparative results are presented in Figure 1. While both water and gelatin remain around the initial temperature after 180 s plasma treatment for kINPen device, plasma treatment using APPJ induces cooling for both samples, with a decrease of 11 ˚C and 12 ˚C for gelatin and water, respectively. To study the contributions of the gas flow on the thermal effects caused on water and gelatin, controls with only gas flow were performed (Supplementary Figure 1). Both devices are fed with high purity dry gas (Ar or He) which induces strong evaporation from the gelatin/water free surface. The thermal energy lost to evaporation induces a cooling of the sample as confirmed by only gas tests. Assuming the enthalpy of water vaporization in gelatin solution is the same as in pure water (2257 J/g), an evaporation of 100 µL over 180 s

results in a cooling power of approximately 1.25 W. On the other side, a portion of the total power consumed by the plasma sources (2.1 W for APPJ and 8.4 W for kINPen on the gelatin solution) is delivered to the target as heat through Joule effect or electromagnetic emission. While for APPJ the cooling effect is stronger than the heating one, for kINPen they are comparable. Both plasma devices warm the samples, but in the case of kINPen, the warming effect is sufficient to counterbalance the cooling effect of evaporation. This can be attributed to the different powers of the two sources.

3.2. Influence of plasma treatment on the generation of RONS in gelatin

Figure 2b & c show the concentration of NO_2^- and H_2O_2 generated in 2% gelatin solution or distilled water as a function of the plasma treatment time, using APPJ or kINPen. Higher amount of NO_2^- and H_2O_2 was measured in 2% gelatin solution compared with water for any of the conditions studied. In both cases of hydrogel or water, production of RONS increases with the plasma treatment time. In DI water, NO_2^- concentration does not further increase after 2-min plasma treatment. Furthermore, production of RONS by kINPen is always higher than using APPJ in 2% gelatin solution and it is equal or higher for water, for similar plasma treatment times.

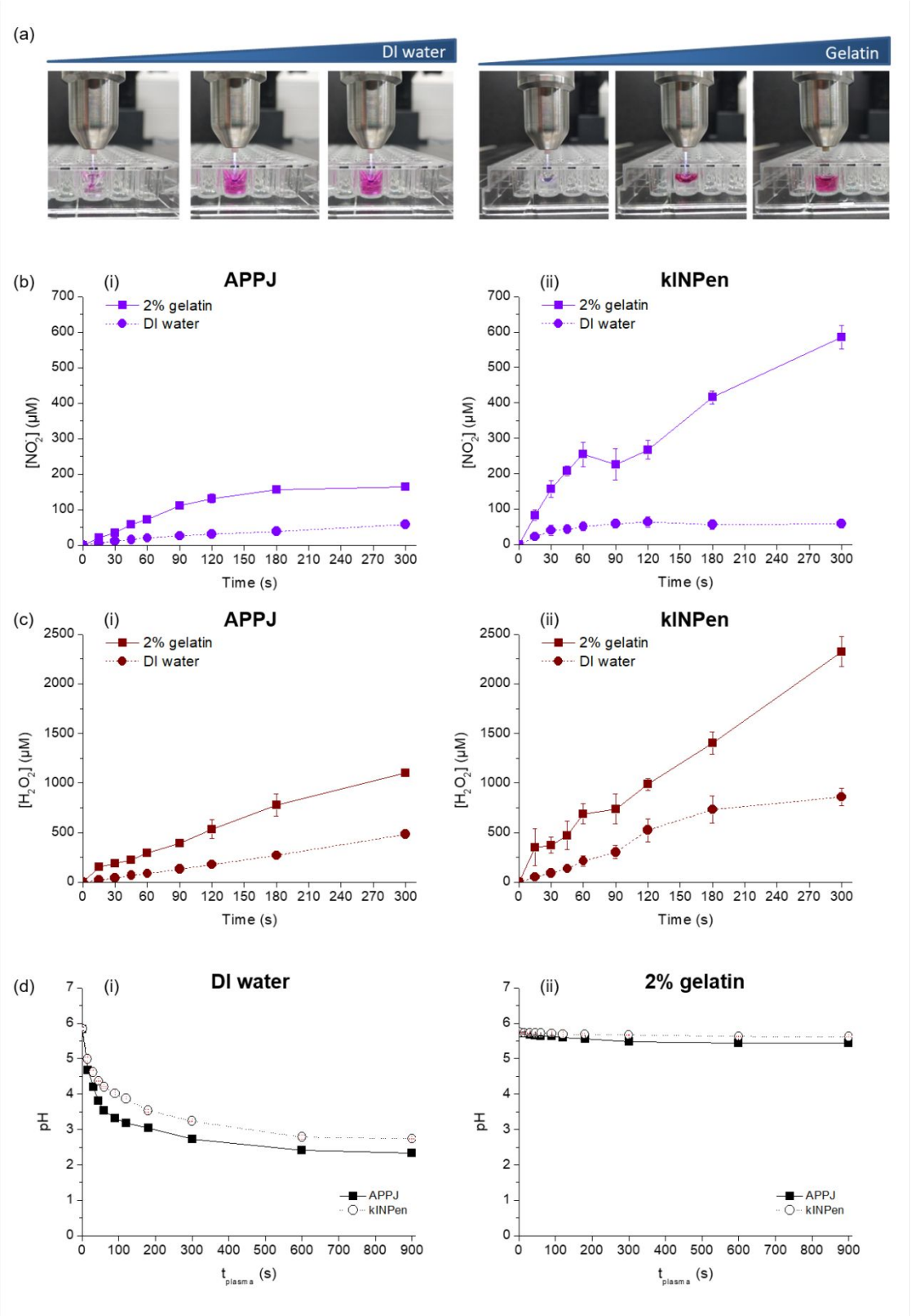

Figure 2. Plasma treatment of distilled water and 2% gelatin solution in presence of Griess reagent for NO_2^- detection (a). Influence of plasma treatment time on NO_2^- (b) and H_2O_2 (c) generation in APPJ- (i) and kINPen-treated (ii) 2% gelatin solution for 10 mm nozzle distance to the liquid surface and 1 L/min gas flow rate, together with the controls in DI water. Monitoring of the pH of 2% gelatin and DI water in the same conditions (d).

The pH of water decreases quickly at short plasma treatment times to below 3 after 900 s of treatment, while the pH of 2% gelatin solution remains between 5.5 and 6 up to 900 s (Figure 2d), highlighting a pH buffering effect of the gelatin.

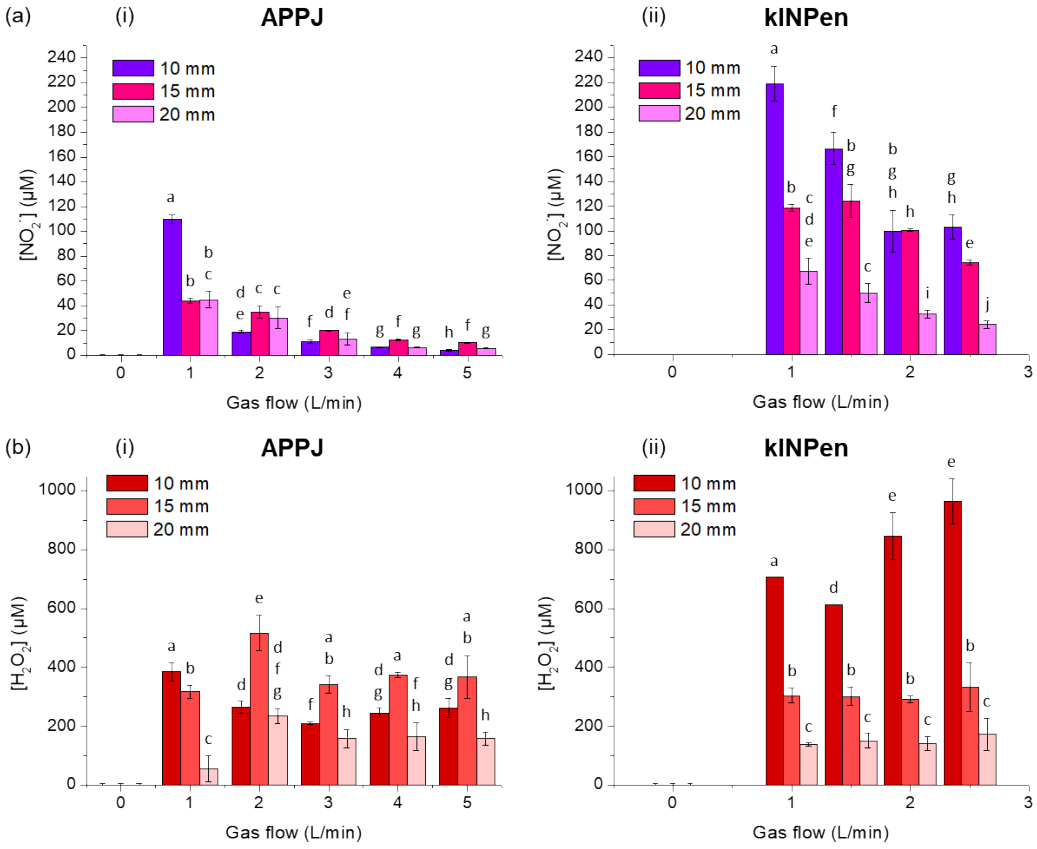

Figure 3. Influence of plasma gas flow rate distance on the concentration of NO_2^- (a) and H_2O_2 (b) from APPJ- and kINPen-treated 2% gelatin for 90 s. Different letters indicate statistically significant differences (mean sd, n=3; p<0.05).

Gas flow rate and distance from the nozzle to the surface of the liquid also play a significant role in the concentration of RONS generated in gelatin (Figure 3a) clearly indicates that higher concentrations of NO_2^- are generated in gelatin solution under low gas flow rate and short nozzle distance. [NO_2^-] is maximized for both plasma devices at 1 L/min of gas flow rate and 10 mm nozzle distance, with concentrations of 112 µM and 219 µM for APPJ and kINPen, respectively. Under the same working conditions, kINPen generates much more nitrites than APPJ for all conditions studied. In contrast, production of H_2O_2 in gelatin (Figure 3b) does not follow the same trend with APPJ with the variation of both nozzle distance and gas flow rates. kINPen displays an increase of H_2O_2 production with the decrease of the nozzle distance, as observed for NO_2^-. In parallel, variation of gas flow does not display variation in the generation of hydrogen peroxides in kINPen-treated gelatin at 15-20 mm but increases at short distance when increasing gas flow rate.

3.3. Stability of RONS in gelatin-based hydrogel

To study the stability of RONS generated in 2% gelatin solution NO_2^- and H_2O_2 were quantified at different times after plasma treatment, at two storage temperatures: 4 °C and 37 °C and compared to DI water as control (Figure 4).

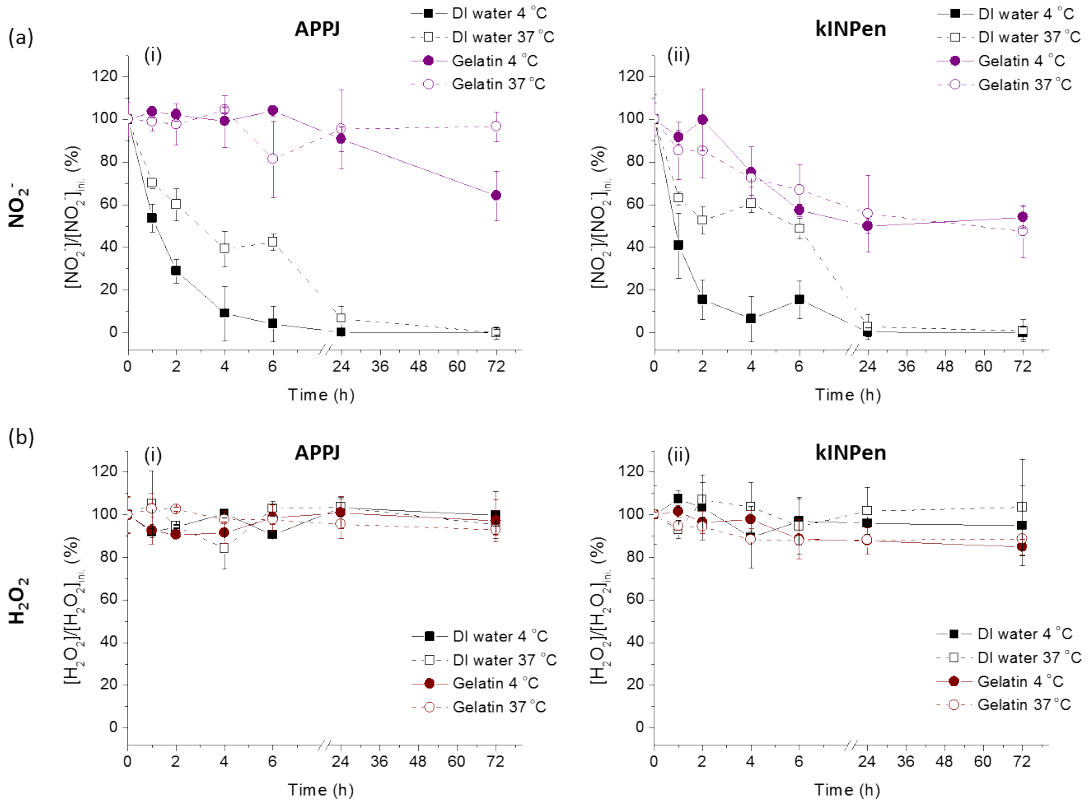

Figure 4: Influence of the storage time and temperature on the ratio of RONS remaining with respect to the initial concentrations of NO_2^- (a) and H_2O_2 (b) in 2% gelatin and water generated by APPJ (left side) and kINPen (right side) plasma treatment (10 mm, 1 L/min, 90 s).

For both APPJ- and kINPen-treated water, a quick decrease of nitrites is observed as a function of the storage time, with a quicker disappearance of NO_2^- at 37 °C than at 4 °C. No nitrite ions were detected in water after 24h. This NO_2^- decreasing trend is slowed down in plasma-treated gelatin, wherein after 24 hours, around 90% and 55% of the initial concentration of NO_2^- remains in the biomaterial (for APPJ and kINPen, respectively). While almost all NO_2^- ions react within the first 24 hours in plasma-treated water, hydrogen peroxides are stable, even after hours. The same stability is observed in plasma-treated 2% gelatin solution, in which H_2O_2 concentration remains constant over 72-hour storage either at 4 °C or 37 °C. To sum up, gelatin hydrogels improve the stability of plasma-generated RONS, as they allow maintaining constant concentration of NO_2^- and H_2O_2 over time.

3.4. Release studies of RONS from plasma-treated hydrogels

The release of NO_2^- and H_2O_2 from the plasma-treated 2% gelatin to PBS (Figure 5) shows a clear dependence of plasma treatment time. Higher release of NO_2^- and H_2O_2 was recorded for longer treatment times, according to the higher initial amount of RONS in the biopolymer. Similarly, the higher amount of RONS generated with kINPen (Figure 2 and Figure 3) result in higher concentrations of nitrites and peroxides released than from the APPJ-treated gelatin solution.

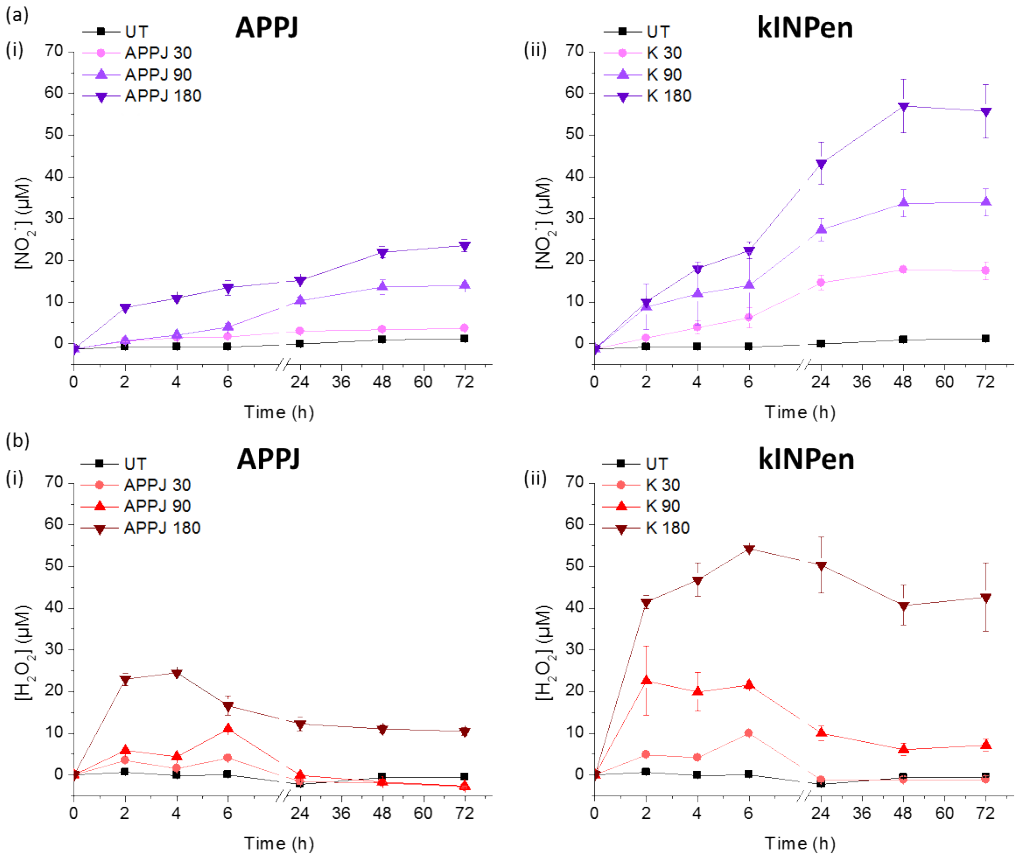

Figure 5. RONS released from APPJ- and kINPen-treated 2% gelatin solution for 30, 90 and 180 s plasma treatment (10 mm, 1 L/min) to PBS release medium: concentration of NO_2^- (a) and H_2O_2 (b). Untreated gelatin solution was employed as control.

3.5. *In vitro* anticancer efficacy

Sarcoma osteogenic SaOS-2 cells were exposed to APPJ- and kINPen-treated 2% gelatin to evaluate the impact on cell viability (Figure 6a). As expected, untreated gelatin is completely biocompatible. The plasma-treated gelatin induced bone cancer cell death, with SaOS-2 cell viability decrease by increasing of treatment time, for both plasma devices tested, but being treatment with kINPen more effective on suppressing viability of osteosarcoma cells. Short plasma treatment times (30 s) already reveal important cytotoxic effects on SaOS-2 cells, with cell viability of 71% for APPJ and 57% for kINPen after 24 hours. Cell viability diminished to 46% and 27% after 24 hours for 180 s APPJ and kINPen treatment, respectively, and further decreased to 23% and 12% after 72 hours. Additionally, while SaOS-2 cells grow homogenously in the well plate when using untreated gelatin, SaOS-2 are killed preferentially just below the insert with the treated gelatin (lack of cells in this area). The diameter of this area of arrested proliferation increases with plasma treatment time, with absence of living cells for longer plasma treatment times in this area (Supplementary Figure 2). It can be assumed that this corresponds to the area of diffusion of RONS nearer the plasma-treated gelatin solution, confirming that the release of RONS is closely linked with the biological effects observed.

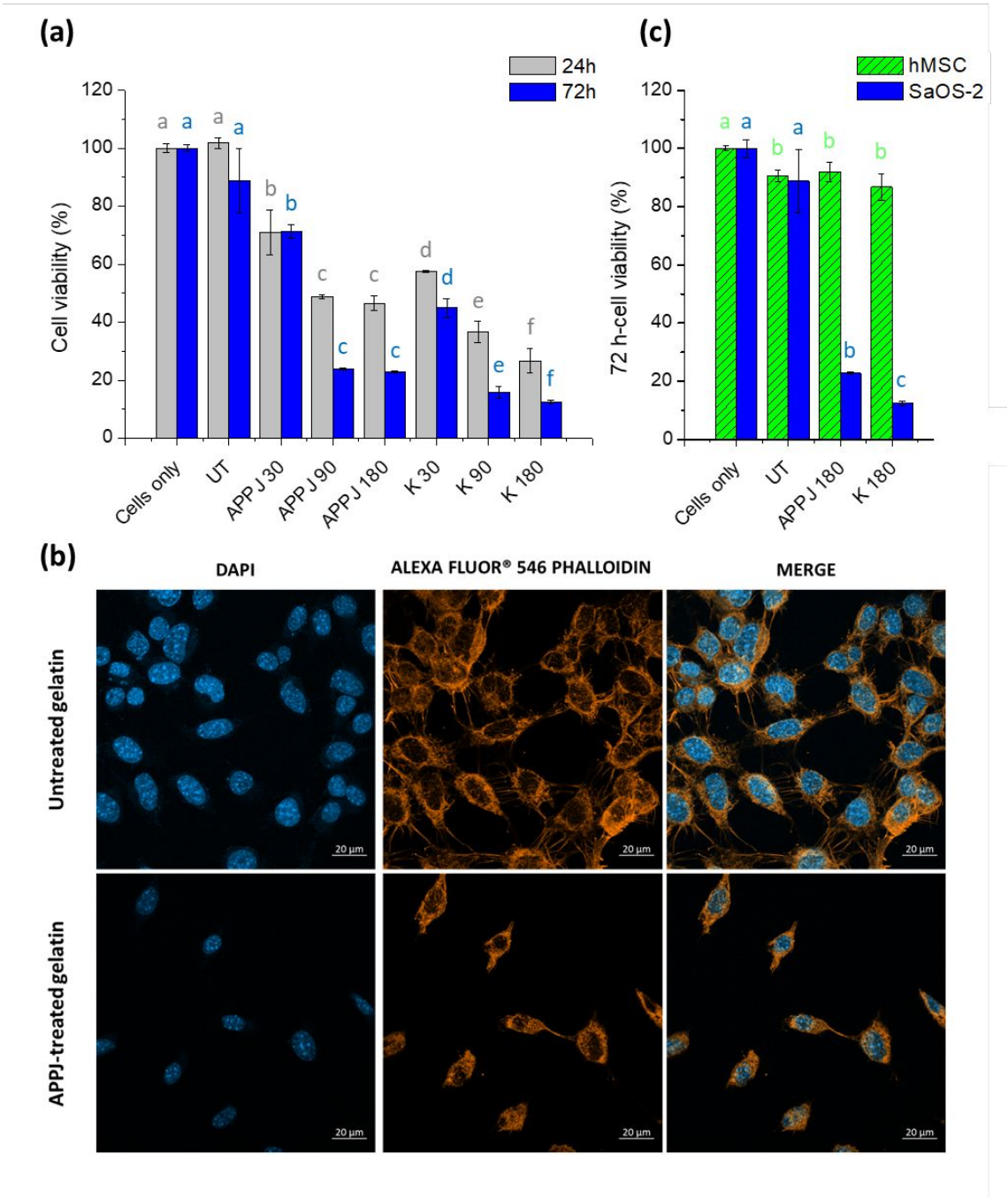

Figure 6. SaOS-2 cell viability after 24 h and 72 h exposition to APPJ) and kINPen (K)-treated 2% gelatin for 30, 90 and 180 s (a). Selectivity of plasma-treated gelatin for 180 s using APPJ and kINPen (10 mm, 1 L/min) (b). Different letters indicate statistically significant differences (mean sd, n=3; p<0.05). Confocal microscopy images of SaOS-2 cells placed for 48 hours in presence of untreated gelatin (control) and APPJ-treated gelatin for 90 s at 1 L/min and 10 mm (c).

Confocal microscopy images (Figure 6b) confirm the previous results; SaOS-2 cells in presence of untreated gelatin display the same morphology than control with cells only. APPJ-treated gelatin induces morphological modifications reflected by a reduction of the expansion or an absence of actin filaments and a reduction of the nuclei size.

Finally, the selectivity of the plasma-treated biomaterial was also tested with hMSC in presence of APPJ and kINPen-treated 2% gelatin solution for 180 seconds as presented in Figure 6c. While

presence of untreated gelatin solution with hMSC confirms the biocompatible behavior of the material with 72-hour cell viability around 91%, the results revealed that plasma treatments of gelatin in the studied conditions have selective effects on cancer cells, maintaining cell viability of healthy cells of 91.9 ± 3.4% and 86.8 ± 4.5% for 180 s APPJ and kINPen treatment, respectively.

4. DISCUSSION

Many studies have shown proof of the anticancer efficacy of plasma-conditioned liquids (PCL) such as physiological saline solutions or culture media[9,10,12,14,42–45]. As alternative to direct treatment of cancer cells by CAP[46,47], that could results more aggressive for healthy cells, the use of PCL presents the advantage of being a minimally-invasive approach with similar *in vitro* results, including better outcomes especially regarding selectivity. However, one of their limitations is that while they can be delivered locally, the liquids can be quickly washed away by body fluids. Here, the production of RONS by plasma jets was enhanced by using a polymer solution of gelatin (Figure 2) with respect to other saline solutions[45] or to the first work evaluating a biopolymer solution of alginate[16]. This opens the door to entrapping these RONS in a biopolymer formulation able to act as vehicle for local delivery of RONS for cancer therapy, potentially allowing extended local therapy with the RONS in the tumor site (Figure 4) rather than the conventional plasma-conditioned saline solutions.

Gelatin has been widely used as carrier material for therapeutic cells and drugs due to their excellent biocompatibility and similarities to the extracellular matrix[48]. To meet the stringent requirements of clinical translation of the hydrogels such preparation, application, mechanical properties, etc. a number of modifications of gelatin have also been investigated[49].

Until now, some works have investigated the diffusion of RONS from plasma jets through gelled (solid) gelatin[34,35,50] and agarose[36,51–54], used as tissue models in plasma medicine. These studies showed that plasma treatment of mm thick gelled gelatin or agarose allow the diffusion of reactive species to a liquid below, as it is thought to happen *in vivo*, with RONS going through the skin.

Our approach here is novel, as we treat liquid gelatin solutions with cold atmospheric plasma jets to generate RONS within it with the aim to include afterward the plasma-treated biopolymer in the design/formulation of a biomaterial able to act as a delivery system.

Different works[55] have investigated the production of RONS in water or saline solutions under a broad range of conditions such as volume, treatment time, gas flow and electrode distance[2,45,51,56–58]. To allow easier extrapolation of results, two plasma jets were employed here. Despite that the great variety of configurations in the plasma literature hamper comparative analysis, it is clear that employing a gelatin solution here leads to much higher generation of RONS. Plasma treatment of the 2% gelatin solution allowed obtaining high concentrations of nitrites and peroxides (Figure 2 & 3). In water (used as control), the concentrations of NO_2^- and H_2O_2 generated agree with those observed in plasma-conditioned water in previous works[55,56] using an APPJ in very similar conditions (20 mm, 100 µL) to those employed here. As in our work, the amount of RONS generated increases with plasma treatment time.

Nevertheless, compared to DI water, the amount of RONS generated in 2% gelatin solution is much higher with any of the two plasma jets investigated here (APPJ or kINPen) (Figure 2). After 3 min of plasma treatment, the amounts of NO_2^- and H_2O_2 generated in gelatin are at least 2

times higher than in water and can reach up to 4.1 and 7.4 fold for NO_2^- with APPJ and kINPen, respectively. This enhanced production of RONS in a biopolymer solution than in water or Ringer's saline was also observed in our previous work with alginate solutions[59]. This difference can be explained by the pH buffering effect of the gelatin solution; while pH decreased with plasma treatment time in Ringer's saline[59] or water (Figure 2d), as also reported in other works[60–62], the pH remained unaltered in buffered saline such as PBS, in alginate[59] or here in gelatin solution. In general, different reactions are fostered in acidic media: NO_2^- reacts with H_2O_2 to form peroxynitrites; nitrous acid – one of the major sources of nitrites - decomposes in acidic media)[4,55,63,64], among other reactions. Since plasma treatment leads to water acidification, these reactions are promoted in water. However, as gelatin solutions are not displaying acidification (Figure 2d) the reactions consuming peroxides and nitrites are slowed down, leading to higher stability of these RONS. While this hypothesis is clearly a common trend between plasma-treated gelatin solution and plasma-treated alginate solution[59], the present work demonstrates that the specific polymer employed to produce the solution is also a keypoint regarding the chemical reactivity of the solution with the plasma gas phase. Gelatin solutions are able to generate several-fold higher concentrations of RONS than alginate solutions (i.e. 226.4 µM of NO_2^- and 740 µM of H_2O_2 were generated in gelatin solution vs. 97.2 µM of NO_2^- and 111.9 µM of H_2O_2, in alginate solution under same conditions - 90 s of kINPen treatment in 200 µL of solution at 10 mm distance and 1 L/min Ar flow rate).

Parameters such as plasma gas flow rate or nozzle distance to the liquid surface can be modified to obtain maximum NO_2^- and H_2O_2 concentrations in the liquids treated. Here we observed that NO_2^- are maximized at short nozzle distance and low gas flow rate, while short distances and high gas flow rates promote higher concentrations of H_2O_2 (Figure 3). As recorded in a previous work, production of RONS is more efficient under same treatment conditions using kINPen than APPJ[59] (Figure 2 and Figure 3). One of the reasons supporting this difference between both devices could lie with the thermal effects observed in Figure 1b that can affect fluid dynamics and thus generation of RONS. While plasma treatment using kINPen is maintaining the temperature of the polymer solution or the water during plasma-treatment for a same gas flow rate and nozzle distance, the cooling down observed with the samples treated with APPJ may affect the diffusion of the reactive species inside the plasma-treated polymer solution due to its higher viscosity, as gelatin starts jellying at temperatures from 25-28 ˚C depending on the concentration and the length of the chain, among others[65]. Lower temperatures revert in a material tending to get a more solid-like behavior, limiting thus the diffusion and generation of RONS inside the polymer network. The difference of behavior in the thermal effects of the samples between APPJ and kINPen most likely arise from the difference of power delivered by both plasma sources. Since the water content in the gas flow is zero in both cases, and thus the contribution of the cooling effect due to evaporation is the same, it can be assumed that the higher power delivered to the plasma discharge by the kINPen (between 0.3 and 3.5 W[66]) with respect to the power delivered by the APPJ (0.3 W measured) is the main reason of the higher counterbalancing in the warming effect presented by the kINPen.

Another important difference between the two sources comes from the type of gas used (He for the APPJ and Ar for the kINPen). Assuming a kinematic viscosity of 1.11×10^{-4} m^2/s for He and of 1.27×10^{-5} m^2/s for Ar, for the gas flow rates (1-5 L/min) and the nozzle diameters (APPJ Ø 1.2 mm, kINPen Ø1.6 mm) adopted in this work the Reynolds number (Re) ranges between 158 and 792 for the APPJ in He and between 1042 and 5200 for the kINPen in Ar. As reported in the literature for a similar jet configuration, a transition from laminar to turbulent flow is expected to occur for Re between 500 and 1000. Thus, it can be assumed that the APPJ operates mostly

in a laminar flow regime while the kINPen in a turbulent one. The turbulent vortexes in the kINPen effluent, while limiting the length of the plasma plume (see in Figure 3 the rapid decrease of RONS with increase of the gap distance), can certainly favor the mixing with surrounding air and therefore allow higher production of RONS with respect to the APPJ[67,68].

Furthermore, the buffering effect observed here in gelatin solution (Figure 2b (i and ii)) may also have two important implications: 1. Cancer cells are known to acidify their environment and, consequently, the interior of the cells themselves is alkalinized. This reverse pH gradient is associated with tumor proliferation, invasion, metastasis, aggressiveness, and treatment resistance[69–75], so the fact of having a buffered delivery vehicle for the plasma-generated RONS (instead of the acidic plasma-treated liquids proposed earlier) might be an advantage which should deserve investigation in future works. 2. A more practical advantage of this pH buffering of gelatin is that it allows the use of the Amplex Red method for detection of H_2O_2, since the HRP enzyme employed in this method remains stable in a pH range between 5.0 and 9.0.

In designing biomaterials, the ability to store them is a practical and important asset in views of future commercialization. Interestingly, storage of plasma-treated DI water and gelatin at 4 ^oC or physiological conditions (37 ^oC) revealed that NO_2^- is more stable in the gelatin solution with respect to water (Figure 4). Whereas almost all the nitrites generated in water disappeared after 24 hours, at least 60% of the initial concentration of nitrites generated in 2% gelatin remained in the material after 72 hours. Meanwhile, H_2O_2 presents a good stability over time up to 72 hours, either for water or gelatin solution, with at least 84.9% of the initial concentration of hydrogen peroxides remaining in gelatin solution after 3-day storage. This trend is not only in accordance with a previous work monitoring storage of H_2O_2 in water over 21 days[60], but above all it highlights a better conservation of H_2O_2 in water or gelatin than observed in cell culture media, such as DMEM[76], where H_2O_2 concentrations reported were 10 times lower after 24 hours.

Release kinetics of NO_2^- and H_2O_2 from APPJ- and kINPen-treated gelatin solution to PBS, clearly show that higher amounts of RONS were released from treated gelatin solution for longer treatment times (Figure 5). A sustained release of NO_2^- can be observed up to 48 hours, whereas H_2O_2 shows burst release, with maximum released after 4-6 hours. While 180 s plasma-treated gelatin solution releases 75% of NO_2^- generated with APPJ and 67% with kINPen after 72 hours, the release percentage of H_2O_2 to PBS is much lower, with values of 7% and 15%, respectively (Supplementary Table 1). However, despite the low release percentage of hydrogen peroxides, the concentrations released allow to observe significant biological effects of SaOS-2 cells (Figure 5).

Osteosarcoma (SaOS-2) cell death was enhanced progressively with plasma-treated gelatin at increasing treatment times (Figure 6a). This can be related to the increasingly higher concentration of RONS produced by plasma jet (Figure 7). This death of cancer cells in a dose-dependent manner has been previously associated with biological and molecular mechanisms of necrosis, apoptosis, senescence, and autophagy triggered by CAP treatment[77]. With [H_2O_2] around 200 µM after 30 s of plasma treatment, cytotoxic effects are already observed with the shortest plasma treatment time. Slightly higher cell cytotoxicity with kINPen than with APPJ can be directly related with the higher amount of RONS generated in the gelatin solution with this plasma jet (Figure 2 and Figure 3). By producing higher amounts of RONS in gelatin than in alginate solutions under the same plasma treatment conditions[16], an important enhancement of cancer cell cytotoxicity is reached by using gelatin solutions, with 72-hour cell viability decreasing down to 12% by using kINPen for 180 s when alginate solutions presented a SaOS-2

cell viability of 62% for the same CAP treatment conditions. This supports to employ preferentially gelatin as biopolymer solution in a further design of CAP-treated biopolymer-based biomaterial to obtained higher loading of RONS and thus, an improve effectiveness in killing cancer cells.

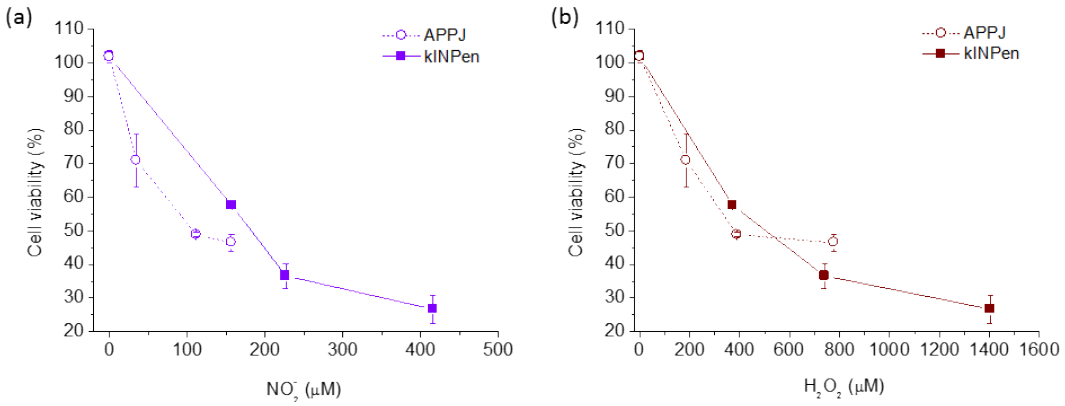

Figure 7: Relationship between NO_2^- (a) and H_2O_2 (b) generated in 2% gelatin solutions and the cytotoxicity observed in SaOS-2 cell viability after 24 hours for APPJ and kINPen treatments (10 mm, 1 L/min).

Morphology and cell density imaged by confocal microscopy (Figure 6b) backup the discussed cellular results for gelatin solution. SaOS-2 osteosarcoma cells in presence of either untreated hydrogels present extended actin filaments and high cell density, accordingly to their suitable biocompatibility (Figure 5a). On the contrary, osteosarcoma cells cultured with plasma-treated gelatin show isolated cells, with fewer adhesion points, smaller nuclei size and more rounded shape, all indicative of the dying fate induced by the plasma-treated biopolymer solutions developed here. Finally, and most importantly, plasma-treated gelatin revealed a selective killing effect on osteosarcoma cells since cell viability of healthy cells (hMSC) is maintained above 90% after 72 hours (Figure 6c). This selective behavior observed with plasma-treated biopolymer solution is in accordance with results obtained in previous works using plasma-conditioned liquids [15,78,79]. As hypothesized for PCL, the mechanism behind this selectivity mainly takes its origin in the difference in basal levels of oxidative stress between healthy and cancer cells lines [8,12]. So, plasma treatment of biopolymer solutions discussed here has several advantages regarding generation and stability of RONS, and above all preserve the biological effects observed with PCL.

5. CONCLUSIONS

Herein we designed and characterized a novel vehicle for atmospheric pressure plasma-generated RONS by comparing two different atmospheric pressure plasma jets. Gelatin solution greatly increases (between 2 and 12-fold) the concentration of RONS produced by cold atmospheric plasma with respect to water. The stability of NO_2^- generated in gelatin was enhanced and that of H_2O_2 was maintained with respect to DI water at least for 72 h. Plasma-treated gelatin solution buffered the pH decrease observed in water which can be an advantage and partially explains the higher RONS measured. Anticancer effects of plasma-treated gelatin solution are time-dependent in SaOS-2 osteosarcoma cells, being closely related with the increase of RONS generated by plasma at longer treatment times that reverts in a higher release

of RONS. Plasma-treated gelatin solution revealed a selective lethality on osteosarcoma cells since cell viability of healthy hMSC cells is maintained above 86% after 72 hours for the longest plasma treatment studied (3 min), while viability of SaOS-2 decreased to 23% and 12% for APPJ and kINPen, respectively. The set of unique features previously described make of gelatin a great candidate for the generation and storage of RONS generated by cold atmospheric plasmas and a relevant material to be used in the design of implantable delivery system, with promising applicability in cancer therapy.

6. ACKNOWLEDGMENTS

This project has received funding from the European Research Council (ERC) under the European Union's Horizon 2020 research and innovation programme (grant agreement No 714793). Authors acknowledge the financial support of MINECO for MAT2015-65601-R project (MINECO/FEDER, EU), for the RyC fellowship of CC and of Generalitat de Catalunya for the SGR2017-1165. Support for the research of MPG was received through the ICREA Academia Award for excellence in research, funded by the Generalitat de Catalunya.

7. REFERENCES

(1) Bruggeman, P. J.; Kushner, M. J.; Locke, B. R.; Gardeniers, J. G. E.; Graham, W. G.; Graves, D. B.; Hofman-Caris, R. C. H. M.; Maric, D.; Reid, J. P.; Ceriani, E.; Fernandez Rivas, D.; Foster, J. E.; Garrick, S. C.; Gorbanev, Y.; Hamaguchi, S.; Iza, F.; Jablonowski, H.; Klimova, E.; Kolb, J.; Krcma, F.; Lukes, P.; MacHala, Z.; Marinov, I.; Mariotti, D.; Mededovic Thagard, S.; Minakata, D.; Neyts, E. C.; Pawlat, J.; Petrovic, Z. L.; Pflieger, R.; Reuter, S.; Schram, D. C.; Schröter, S.; Shiraiwa, M.; Tarabová, B.; Tsai, P. A.; Verlet, J. R. R.; Von Woedtke, T.; Wilson, K. R.; Yasui, K.; Zvereva, G. Plasma-Liquid Interactions: A Review and Roadmap. *Plasma Sources Science and Technology*. 2016. https://doi.org/10.1088/0963-0252/25/5/053002.

(2) Chauvin, J.; Judée, F.; Yousfi, M.; Vicendo, P.; Merbahi, N. Analysis of Reactive Oxygen and Nitrogen Species Generated in Three Liquid Media by Low Temperature Helium Plasma Jet. *Sci. Rep.* **2017**. https://doi.org/10.1038/s41598-017-04650-4.

(3) Verlackt, C. C. W.; Van Boxem, W.; Bogaerts, A. Transport and Accumulation of Plasma Generated Species in Aqueous Solution. *Phys. Chem. Chem. Phys.* **2018**, *20* (10), 6845–6859. https://doi.org/10.1039/C7CP07593F.

(4) Machala, Z.; Tarabova, B.; Hensel, K.; Spetlikova, E.; Sikurova, L.; Lukes, P. Formation of ROS and RNS in Water Electro-Sprayed through Transient Spark Discharge in Air and Their Bactericidal Effects. *Plasma Process. Polym.* **2013**. https://doi.org/10.1002/ppap.201200113.

(5) Yilmazer, A. Cancer Cell Lines Involving Cancer Stem Cell Populations Respond to Oxidative Stress. *Biotechnol. reports (Amsterdam, Netherlands)* **2017**, *17*, 24–30. https://doi.org/10.1016/j.btre.2017.11.004.

(6) Reuter, S.; Gupta, S. C.; Chaturvedi, M. M.; Aggarwal, B. B. Oxidative Stress,

Inflammation, and Cancer: How Are They Linked? *Free Radic. Biol. Med.* **2010**, *49* (11), 1603–1616. https://doi.org/10.1016/j.freeradbiomed.2010.09.006.

(7) Schumacker, P. T. Reactive Oxygen Species in Cancer: A Dance with the Devil. *Cancer Cell* **2015**, *27* (2), 156–157. https://doi.org/10.1016/j.ccell.2015.01.007.

(8) Trachootham, D.; Alexandre, J.; Huang, P. Targeting Cancer Cells by ROS-Mediated Mechanisms: A Radical Therapeutic Approach? *Nat. Rev. Drug Discov.* **2009**, *8*, 579.

(9) Van Boxem, W.; Van Der Paal, J.; Gorbanev, Y.; Vanuytsel, S.; Smits, E.; Dewilde, S.; Bogaerts, A. Anti-Cancer Capacity of Plasma-Treated PBS: Effect of Chemical Composition on Cancer Cell Cytotoxicity. *Sci. Rep.* **2017**. https://doi.org/10.1038/s41598-017-16758-8.

(10) Keidar, M. Plasma for Cancer Treatment. *Plasma Sources Sci. Technol.* **2015**, *24* (3), 33001.

(11) Keidar, M.; Shashurin, A.; Volotskova, O.; Ann Stepp, M.; Srinivasan, P.; Sandler, A.; Trink, B. Cold Atmospheric Plasma in Cancer Therapy. *Phys. Plasmas* **2013**. https://doi.org/10.1063/1.4801516.

(12) Yan, D.; Talbot, A.; Nourmohammadi, N.; Sherman, J. H.; Cheng, X.; Keidar, M. Toward Understanding the Selective Anticancer Capacity of Cold Atmospheric Plasma—A Model Based on Aquaporins (Review). *Biointerphases* **2015**, *10* (4), 40801. https://doi.org/10.1116/1.4938020.

(13) Yan, D.; Sherman, J. H.; Keidar, M. Cold Atmospheric Plasma, a Novel Promising Anti-Cancer Treatment Modality. *Oncotarget* **2017**. https://doi.org/10.18632/oncotarget.13304.

(14) Tanaka, H.; Nakamura, K.; Mizuno, M.; Ishikawa, K.; Takeda, K.; Kajiyama, H.; Utsumi, F.; Kikkawa, F.; Hori, M. Non-Thermal Atmospheric Pressure Plasma Activates Lactate in Ringer's Solution for Anti-Tumor Effects. *Sci. Rep.* **2016**, *6* (1), 36282. https://doi.org/10.1038/srep36282.

(15) Canal, C.; Fontelo, R.; Hamouda, I.; Guillem-Marti, J.; Cvelbar, U.; Ginebra, M. P. Plasma-Induced Selectivity in Bone Cancer Cells Death. *Free Radic. Biol. Med.* **2017**. https://doi.org/10.1016/j.freeradbiomed.2017.05.023.

(16) Labay, C.; Hamouda, I.; Tampieri, F.; Ginebra, M.-P.; Canal, C. Production of Reactive Species in Alginate Hydrogels for Cold Atmospheric Plasma-Based Therapies. *Sci. Rep.* **2019**, *9* (1), 16160. https://doi.org/10.1038/s41598-019-52673-w.

(17) Echave, M. C.; Saenz del Burgo, L.; Pedraz, J. L.; Orive, G. Gelatin as Biomaterial for Tissue Engineering. *Curr. Pharm. Des.* **2017**, *23* (24), 3567–3584. https://doi.org/10.2174/1381612823666170511123101.

(18) Esposito, E.; Cortesi, R.; Nastruzzi, C. Gelatin Microspheres: Influence of Preparation Parameters and Thermal Treatment on Chemico-Physical and Biopharmaceutical Properties. *Biomaterials* **1996**, *17* (20), 2009–2020. https://doi.org/https://doi.org/10.1016/0142-9612(95)00325-8.

(19) Solorio, L.; Zwolinski, C.; Lund, A. W.; Farrell, M. J.; Stegemann, J. P. Gelatin Microspheres Crosslinked with Genipin for Local Delivery of Growth Factors. *J. Tissue Eng. Regen. Med.* **2010**, *4* (7), 514–523. https://doi.org/10.1002/term.267.

(20) Rose, J. C. B. and M. A. and G. E. M. and N. R. W. M. and D. J. P. and A. J. K. and J. W. A.

and M. P. L. and F. R. A. J. Electrospun Gelatin-Based Scaffolds as a Novel 3D Platform to Study the Function of Contractile Smooth Muscle Cells in Vitro. *Biomed. Phys. Eng. Express* **2018**, *4* (4), 45039.

(21) Poursamar, S. A.; Hatami, J.; Lehner, A. N.; da Silva, C. L.; Ferreira, F. C.; Antunes, A. P. M. Potential Application of Gelatin Scaffolds Prepared through in Situ Gas Foaming in Skin Tissue Engineering. *Int. J. Polym. Mater. Polym. Biomater.* **2016**, *65* (6), 315–322. https://doi.org/10.1080/00914037.2015.1119688.

(22) Tan, J. Y.; Chua, C. K.; Leong, K. F. Indirect Fabrication of Gelatin Scaffolds Using Rapid Prototyping Technology. *Virtual Phys. Prototyp.* **2010**, *5* (1), 45–53. https://doi.org/10.1080/17452751003759144.

(23) Rose, J. B.; Pacelli, S.; Haj, A. J. El; Dua, H. S.; Hopkinson, A.; White, L. J.; Rose, F. R. A. J. Gelatin-Based Materials in Ocular Tissue Engineering. *Mater. (Basel, Switzerland)* **2014**, *7* (4), 3106–3135. https://doi.org/10.3390/ma7043106.

(24) Phull, M. K.; Eydmann, T.; Roxburgh, J.; Sharpe, J. R.; Lawrence-Watt, D. J.; Phillips, G.; Martin, Y. Novel Macro-Microporous Gelatin Scaffold Fabricated by Particulate Leaching for Soft Tissue Reconstruction with Adipose-Derived Stem Cells. *J. Mater. Sci. Mater. Med.* **2013**, *24* (2), 461–467. https://doi.org/10.1007/s10856-012-4806-0.

(25) Aliakbarshirazi, S.; Talebian, A. Electrospun Gelatin Nanofibrous Scaffolds for Cartilage Tissue Engineering. *Mater. Today Proc.* **2017**, *4* (7, Part 1), 7059–7064. https://doi.org/https://doi.org/10.1016/j.matpr.2017.07.038.

(26) Aldana, A. A.; Abraham, G. A. Current Advances in Electrospun Gelatin-Based Scaffolds for Tissue Engineering Applications. *Int. J. Pharm.* **2017**, *523* (2), 441–453. https://doi.org/10.1016/j.ijpharm.2016.09.044.

(27) Dias, J. R.; Baptista-Silva, S.; Oliveira, C. M. T. de; Sousa, A.; Oliveira, A. L.; Bártolo, P. J.; Granja, P. L. In Situ Crosslinked Electrospun Gelatin Nanofibers for Skin Regeneration. *Eur. Polym. J.* **2017**, *95*, 161–173. https://doi.org/https://doi.org/10.1016/j.eurpolymj.2017.08.015.

(28) Fassina, L.; Saino, E.; Visai, L.; Avanzini, M. A.; Cusella De Angelis, M. G.; Benazzo, F.; Van Vlierberghe, S.; Dubruel, P.; Magenes, G. Use of a Gelatin Cryogel as Biomaterial Scaffold in the Differentiation Process of Human Bone Marrow Stromal Cells. *Conf. Proc. ... Annu. Int. Conf. IEEE Eng. Med. Biol. Soc. IEEE Eng. Med. Biol. Soc. Annu. Conf.* **2010**, *2010*, 247–250. https://doi.org/10.1109/IEMBS.2010.5627475.

(29) Zhang, Y.; Ouyang, H.; Lim, C. T.; Ramakrishna, S.; Huang, Z.-M. Electrospinning of Gelatin Fibers and Gelatin/PCL Composite Fibrous Scaffolds. *J. Biomed. Mater. Res. B. Appl. Biomater.* **2005**, *72* (1), 156–165. https://doi.org/10.1002/jbm.b.30128.

(30) Raina, D. B.; Larsson, D.; Mrkonjic, F.; Isaksson, H.; Kumar, A.; Lidgren, L.; Tägil, M. Gelatin- Hydroxyapatite- Calcium Sulphate Based Biomaterial for Long Term Sustained Delivery of Bone Morphogenic Protein-2 and Zoledronic Acid for Increased Bone Formation: In-Vitro and in-Vivo Carrier Properties. *J. Control. Release* **2018**, *272*, 83–96. https://doi.org/https://doi.org/10.1016/j.jconrel.2018.01.006.

(31) Kessler, L.; Gehrke, S.; Winnefeld, M.; Huber, B.; Hoch, E.; Walter, T.; Wyrwa, R.; Schnabelrauch, M.; Schmidt, M.; Kückelhaus, M.; Lehnhardt, M.; Hirsch, T.; Jacobsen, F. Methacrylated Gelatin/Hyaluronan-Based Hydrogels for Soft Tissue Engineering. *J. Tissue Eng.* **2017**, *8*, 2041731417744157–2041731417744157. https://doi.org/10.1177/2041731417744157.

(32) Gattazzo, F.; De Maria, C.; Rimessi, A.; Dona, S.; Braghetta, P.; Pinton, P.; Vozzi, G.; Bonaldo, P. Gelatin-Genipin-Based Biomaterials for Skeletal Muscle Tissue Engineering. *J. Biomed. Mater. Res. B. Appl. Biomater.* **2018**, *106* (8), 2763–2777. https://doi.org/10.1002/jbm.b.34057.

(33) Szili, S. E. M. and A. T. A. J. and S. A. A.-B. and R. D. S. and S.-H. H. and N. T. T. and J.-S. O. and J. W. B. and E. J. Studying the Cytolytic Activity of Gas Plasma with Self-Signalling Phospholipid Vesicles Dispersed within a Gelatin Matrix. *J. Phys. D. Appl. Phys.* **2013**, *46* (18), 185401.

(34) Short, E. J. S. and J. W. B. and R. D. A 'Tissue Model' to Study the Plasma Delivery of Reactive Oxygen Species. *J. Phys. D. Appl. Phys.* **2014**, *47* (15), 152002.

(35) Gaur, N.; Szili, E. J.; Oh, J.-S.; Hong, S.-H.; Michelmore, A.; Graves, D. B.; Hatta, A.; Short, R. D. Combined Effect of Protein and Oxygen on Reactive Oxygen and Nitrogen Species in the Plasma Treatment of Tissue. *Appl. Phys. Lett.* **2015**, *107* (10), 103703. https://doi.org/10.1063/1.4930874.

(36) Short, E. J. S. and J.-S. O. and S.-H. H. and A. H. and R. D. Probing the Transport of Plasma-Generated RONS in an Agarose Target as Surrogate for Real Tissue: Dependency on Time, Distance and Material Composition. *J. Phys. D. Appl. Phys.* **2015**, *48* (20), 202001.

(37) Szili, E. J.; Hong, S.-H.; Short, R. D. On the Effect of Serum on the Transport of Reactive Oxygen Species across Phospholipid Membranes. *Biointerphases* **2015**, *10* (2), 29511. https://doi.org/10.1116/1.4918765.

(38) Zaplotnik, R.; Bišćan, M.; Kregar, Z.; Cvelbar, U.; Mozetič, M.; Milošević, S. Influence of a Sample Surface on Single Electrode Atmospheric Plasma Jet Parameters. *Spectrochim. Acta Part B At. Spectrosc.* **2015**, *103–104*, 124–130. https://doi.org/https://doi.org/10.1016/j.sab.2014.12.004.

(39) Reuter, S.; von Woedtke, T.; Weltmann, K.-D. The KINPen—a Review on Physics and Chemistry of the Atmospheric Pressure Plasma Jet and Its Applications. *J. Phys. D. Appl. Phys.* **2018**, *51* (23), 233001.

(40) Guevara, I.; Iwanejko, J.; Dembinska-Kiec, A.; Pankiewicz, J.; Wanat, A.; Anna, P.; Golabek, I.; Bartus, S.; Malczewska-Malec, M.; Szczudlik, A. Determination of Nitrite/Nitrate in Human Biological Material by the Simple Griess Reaction. *Clin. Chim. Acta.* **1998**, *274* (2), 177–188.

(41) Giustarini, D.; Rossi, R.; Milzani, A.; Dalle-Donne, I. Nitrite and Nitrate Measurement by Griess Reagent in Human Plasma: Evaluation of Interferences and Standardization. *Methods Enzymol.* **2008**, *440*, 361–380. https://doi.org/10.1016/S0076-6879(07)00823-3.

(42) Kaushik, N. K.; Ghimire, B.; Li, Y.; Adhikari, M.; Veerana, M.; Kaushik, N.; Jha, N.; Adhikari, B.; Lee, S.-J.; Masur, K.; von Woedtke, T.; Weltmann, K.-D.; Choi, E. H. Biological and Medical Applications of Plasma-Activated Media, Water and Solutions. *Biol. Chem.* **2018**, *400* (1), 39–62. https://doi.org/10.1515/hsz-2018-0226.

(43) Azzariti, A.; Iacobazzi, R. M.; Di Fonte, R.; Porcelli, L.; Gristina, R.; Favia, P.; Fracassi, F.; Trizio, I.; Silvestris, N.; Guida, G.; Tommasi, S.; Sardella, E. Plasma-Activated Medium Triggers Cell Death and the Presentation of Immune Activating Danger Signals in Melanoma and Pancreatic Cancer Cells. *Sci. Rep.* **2019**, *9* (1), 4099. https://doi.org/10.1038/s41598-019-40637-z.

(44) Liedtke, K. R.; Bekeschus, S.; Kaeding, A.; Hackbarth, C.; Kuehn, J.-P.; Heidecke, C.-D.; von Bernstorff, W.; von Woedtke, T.; Partecke, L. I. Non-Thermal Plasma-Treated Solution Demonstrates Antitumor Activity against Pancreatic Cancer Cells in Vitro and in Vivo. *Sci. Rep.* **2017**, *7* (1), 8319. https://doi.org/10.1038/s41598-017-08560-3.

(45) Mateu-Sanz, M.; Tornín, J.; Brulin, B.; Khlyustova, A.; Ginebra, M.-P.; Layrolle, P.; Canal, C. Cold Plasma-Treated Ringer's Saline: A Weapon to Target Osteosarcoma. *Cancers (Basel).* **2020**, *12* (1), 227. https://doi.org/10.3390/cancers12010227.

(46) Yan, D.; Wang, Q.; Adhikari, M.; Malyavko, A.; Lin, L.; Zolotukhin, D.; Yao, X.; Kirschner, M.; Sherman, J. H.; Keidar, M. A Physically Triggered Cell Death via Transbarrier Cold Atmospheric Plasma Cancer Treatment. *ACS Appl. Mater. Interfaces* **2020**. https://doi.org/10.1021/acsami.0c06500.

(47) Gjika, E.; Pal-Ghosh, S.; Tang, A.; Kirschner, M.; Tadvalkar, G.; Canady, J.; Stepp, M. A.; Keidar, M. Adaptation of Operational Parameters of Cold Atmospheric Plasma for in Vitro Treatment of Cancer Cells. *ACS Appl. Mater. Interfaces* **2018**, *10* (11), 9269–9279. https://doi.org/10.1021/acsami.7b18653.

(48) Xu, J.; Feng, Q.; Lin, S.; Yuan, W.; Li, R.; Li, J.; Wei, K.; Chen, X.; Zhang, K.; Yang, Y.; Wu, T.; Wang, B.; Zhu, M.; Guo, R.; Li, G.; Bian, L. Injectable Stem Cell-Laden Supramolecular Hydrogels Enhance in Situ Osteochondral Regeneration via the Sustained Co-Delivery of Hydrophilic and Hydrophobic Chondrogenic Molecules. *Biomaterials* **2019**. https://doi.org/https://doi.org/10.1016/j.biomaterials.2019.04.031.

(49) Feng, Q.; Wei, K.; Lin, S.; Xu, Z.; Sun, Y.; Shi, P.; Li, G.; Bian, L. Mechanically Resilient, Injectable, and Bioadhesive Supramolecular Gelatin Hydrogels Crosslinked by Weak Host-Guest Interactions Assist Cell Infiltration and in Situ Tissue Regeneration. *Biomaterials* **2016**, *101*, 217–228. https://doi.org/https://doi.org/10.1016/j.biomaterials.2016.05.043.

(50) Kong, T. H. and D. L. and H. X. and Z. liu and D. X. and D. L. and Q. L. and M. R. and M. G. A 'Tissue Model' to Study the Barrier Effects of Living Tissues on the Reactive Species Generated by Surface Air Discharge. *J. Phys. D. Appl. Phys.* **2016**, *49* (20), 205204.

(51) Oh, J.-S.; Szili, E. J.; Ito, S.; Hong, S.-H.; Gaur, N.; Furuta, H.; Short, R. D.; Hatta, A. Slow Molecular Transport of Plasma-Generated Reactive Oxygen and Nitrogen Species and O2 through Agarose as a Surrogate for Tissue. *Plasma Med.* **2015**. https://doi.org/10.1615/PlasmaMed.2016015740.

(52) Oh, J.-S.; Szili, E. J.; Gaur, N.; Hong, S.-H.; Furuta, H.; Kurita, H.; Mizuno, A.; Hatta, A.; Short, R. D. How to Assess the Plasma Delivery of RONS into Tissue Fluid and Tissue. *J. Phys. D. Appl. Phys.* **2016**, *49* (30), 304005. https://doi.org/10.1088/0022-3727/49/30/304005.

(53) Kawasaki, T.; Sato, A.; Kusumegi, S.; Kudo, A.; Sakanoshita, T.; Tsurumaru, T.; Uchida, G.; Koga, K.; Shiratani, M. Two-Dimensional Concentration Distribution of Reactive Oxygen Species Transported through a Tissue Phantom by Atmospheric-Pressure Plasma-Jet Irradiation. *Appl. Phys. Express* **2016**, *9* (7), 76202. https://doi.org/10.7567/apex.9.076202.

(54) Oh, J.-S.; Szili, E. J.; Gaur, N.; Hong, S.-H.; Furuta, H.; Short, R. D.; Hatta, A. In-Situ UV Absorption Spectroscopy for Monitoring Transport of Plasma Reactive Species through Agarose as Surrogate for Tissue. *J. Photopolym. Sci. Technol.* **2015**, *28* (3), 439–444. https://doi.org/10.2494/photopolymer.28.439.

(55) Khlyustova, A.; Labay, C.; Machala, Z.; Ginebra, M.-P.; Canal, C. Important Parameters in Plasma Jets for the Production of RONS in Liquids for Plasma Medicine: A Brief Review. *Front. Chem. Sci. Eng.* **2019**. https://doi.org/10.1007/s11705-019-1801-8.

(56) Chen, Z.; Simonyan, H.; Cheng, X.; Gjika, E.; Lin, L.; Canady, J.; Sherman, J. H.; Young, C.; Keidar, M. A Novel Micro Cold Atmospheric Plasma Device for Glioblastoma Both in Vitro and in Vivo. *Cancers (Basel).* **2017**. https://doi.org/10.3390/cancers9060061.

(57) Attri, P.; Yusupov, M.; Park, J. H.; Lingamdinne, L. P.; Koduru, J. R.; Shiratani, M.; Choi, E. H.; Bogaerts, A. Mechanism and Comparison of Needle-Type Non-Thermal Direct and Indirect Atmospheric Pressure Plasma Jets on the Degradation of Dyes. *Sci. Rep.* **2016**. https://doi.org/10.1038/srep34419.

(58) Oh, J.-S.; Szili, E. J.; Ogawa, K.; Short, R. D.; Ito, M.; Furuta, H.; Hatta, A. UV–Vis Spectroscopy Study of Plasma-Activated Water: Dependence of the Chemical Composition on Plasma Exposure Time and Treatment Distance. *Jpn. J. Appl. Phys.* **2018**, *57* (1), 0102B9. https://doi.org/10.7567/JJAP.57.0102B9.

(59) Labay, Cédric; Hamouda, Inès; Tampieri, Francesco; Ginebra, Maria-Pau; Canal, C. Production of Reactive Species in Alginate Hydrogels for Cold Atmospheric Plasma-Based Therapies. *Sci. Rep.* **2019**.

(60) Vlad, I.-E.; Anghel, S. D. Time Stability of Water Activated by Different On-Liquid Atmospheric Pressure Plasmas. *J. Electrostat.* **2017**, *87*, 284–292. https://doi.org/https://doi.org/10.1016/j.elstat.2017.06.002.

(61) Zhou, R.; Zhou, R.; Prasad, K.; Fang, Z.; Speight, R.; Bazaka, K.; Ostrikov, K. (Ken). Cold Atmospheric Plasma Activated Water as a Prospective Disinfectant: The Crucial Role of Peroxynitrite. *Green Chem.* **2018**, *20* (23), 5276–5284. https://doi.org/10.1039/C8GC02800A.

(62) Abuzairi, T.; Ramadhanty, S.; Puspohadiningrum, D. F.; Ratnasari, A.; Poespawati, N. R.; Purnamaningsih, R. W. Investigation on Physicochemical Properties of Plasma-Activated Water for the Application of Medical Device Sterilization. *AIP Conf. Proc.* **2018**, *1933* (1), 40017. https://doi.org/10.1063/1.5023987.

(63) Bosi, F. J.; Tampieri, F.; Marotta, E.; Bertani, R.; Pavarin, D.; Paradisi, C. Characterization and Comparative Evaluation of Two Atmospheric Plasma Sources for Water Treatment. *Plasma Process. Polym.* **2018**, *15* (3), 1700130. https://doi.org/10.1002/ppap.201700130.

(64) Clupek, P. L. and E. D. and I. S. and M. Aqueous-Phase Chemistry and Bactericidal Effects from an Air Discharge Plasma in Contact with Water: Evidence for the Formation of Peroxynitrite through a Pseudo-Second-Order Post-Discharge Reaction of H 2 O 2 and HNO 2. *Plasma Sources Sci. Technol.* **2014**, *23* (1), 15019.

(65) Tosh, S. M.; Marangoni, A. G. Determination of the Maximum Gelation Temperature in Gelatin Gels. *Appl. Phys. Lett.* **2004**, *84* (21), 4242–4244. https://doi.org/10.1063/1.1756210.

(66) Reuter, S.; von Woedtke, T.; Weltmann, K.-D. The KINPen—a Review on Physics and Chemistry of the Atmospheric Pressure Plasma Jet and Its Applications. *J. Phys. D. Appl. Phys.* **2018**, *51* (23), 233001.

(67) Stancampiano, A.; Simoncelli, E.; Boselli, M.; Colombo, V.; Gherardi, M. Experimental Investigation on the Interaction of a Nanopulsed Plasma Jet with a Liquid Target.

Plasma Sources Sci. Technol. **2018**, *27* (12), 125002. https://doi.org/10.1088/1361-6595/aae9d0.

(68) Ungate, C.; Harleman, D.; Jirka, G. Stability and Mixing of Submerged Turbulent Jets at Low Reynolds Numbers. *MIT Dep Civ Eng Ralph M, Parsons Lab Water Resour Hydrodyn Rep* **1975**.

(69) Persi, E.; Duran-Frigola, M.; Damaghi, M.; Roush, W. R.; Aloy, P.; Cleveland, J. L.; Gillies, R. J.; Ruppin, E. Systems Analysis of Intracellular PH Vulnerabilities for Cancer Therapy. *Nat. Commun.* **2018**, *9* (1), 2997. https://doi.org/10.1038/s41467-018-05261-x.

(70) Schulze, A.; Harris, A. L. How Cancer Metabolism Is Tuned for Proliferation and Vulnerable to Disruption. *Nature* **2012**, *491*, 364.

(71) Webb, B. A.; Chimenti, M.; Jacobson, M. P.; Barber, D. L. Dysregulated PH: A Perfect Storm for Cancer Progression. *Nat. Rev. Cancer* **2011**, *11*, 671.

(72) Gatenby, R. A.; Gillies, R. J. Why Do Cancers Have High Aerobic Glycolysis? *Nat. Rev. Cancer* **2004**, *4* (11), 891–899. https://doi.org/10.1038/nrc1478.

(73) Gatenby, R. A.; Gawlinski, E. T.; Gmitro, A. F.; Kaylor, B.; Gillies, R. J. Acid-Mediated Tumor Invasion: A Multidisciplinary Study. *Cancer Res.* **2006**, *66* (10), 5216 LP – 5223. https://doi.org/10.1158/0008-5472.CAN-05-4193.

(74) Robey, I. F.; Baggett, B. K.; Kirkpatrick, N. D.; Roe, D. J.; Dosescu, J.; Sloane, B. F.; Hashim, A. I.; Morse, D. L.; Raghunand, N.; Gatenby, R. A.; Gillies, R. J. Bicarbonate Increases Tumor PH and Inhibits Spontaneous Metastases. *Cancer Res.* **2009**, *69* (6), 2260 LP – 2268. https://doi.org/10.1158/0008-5472.CAN-07-5575.

(75) McCarty, M. F.; Whitaker, J. Manipulating Tumor Acidification as a Cancer Treatment Strategy. *Altern. Med. Rev.* **2010**, *15* (3), 264–272.

(76) Hoentsch, M.; Bussiahn, R.; Rebl, H.; Bergemann, C.; Eggert, M.; Frank, M.; von Woedtke, T.; Nebe, B. Persistent Effectivity of Gas Plasma-Treated, Long Time-Stored Liquid on Epithelial Cell Adhesion Capacity and Membrane Morphology. *PLoS One* **2014**, *9* (8), e104559.

(77) Semmler, M. L.; Bekeschus, S.; Schäfer, M.; Bernhardt, T.; Fischer, T.; Witzke, K.; Seebauer, C.; Rebl, H.; Grambow, E.; Vollmar, B.; Nebe, J. B.; Metelmann, H.-R.; Woedtke, T. von; Emmert, S.; Boeckmann, L. Molecular Mechanisms of the Efficacy of Cold Atmospheric Pressure Plasma (CAP) in Cancer Treatment. *Cancers (Basel).* **2020**, *12* (2), 269. https://doi.org/10.3390/cancers12020269.

(78) Laroussi, M. Effects of PAM on Select Normal and Cancerous Epithelial Cells. *Plasma Res. Express* **2019**, *1* (2), 25010. https://doi.org/10.1088/2516-1067/ab1b8a.

(79) Xiang, L.; Xu, X.; Zhang, S.; Cai, D.; Dai, X. Cold Atmospheric Plasma Conveys Selectivity on Triple Negative Breast Cancer Cells Both in Vitro and in Vivo. *Free Radic. Biol. Med.* **2018**, *124*, 205–213. https://doi.org/10.1016/j.freeradbiomed.2018.06.001.

All authors have approved the submitted version;

All authors have agreed both to be personally accountable for the author's own contributions and to ensure that questions related to the accuracy or integrity of any part of the work, even ones in which the author was not personally involved, are appropriately investigated, resolved, and the resolution documented in the literature.

Declaration of interests

Following the competing interests statement guidelines of the publication, the authors declare no competing interests.